24th COBEM - 2017

24th ABCM International Congress of Mechanical Engineering
December 3-8, 2017, Curitiba, PR, Brazil

COBEM-2017-0040
GAS-SOLID FLOWS IN HORIZONTAL PIPES WITH ROUGH AND SMOOTH WALLS

Diego Nei Venturi
Francisco José de Souza
School of Mechanical Engineering, Federal University of Uberlândia, 2121 João Naves de Ávila Ave., Building 5P, Uberlândia, Minas Gerais, 38400-902, Brazil
diegoventuri@gmail.com, francisco.souza@ufu.br

Abstract. *As gas-solid flows are present in many industrial applications, the importance of its simulation grows bigger. The in-house code UNSCYFL3D is used to simulate four horizontal pipe gas-solid flow cases evaluating the influence of rough and smooth wall surfaces. Inter-particle collisions are handles stochastically. Results show the importance of correctly estimating the wall collision parameters and that the methodology is suitable for the simulations, with the exception of one case, which reasons for poor agreement are unclear.*

Keywords: *particle, collision, roughness, wall, flow.*

1. INTRODUCTION

Gas-solid flows are of great concern for many engineering applications, such as in erosion prediction (Duarte et al., 2016; Sedrez et al., 2017), design and optimizations of cyclone separators (de Souza et al., 2012; Sgrott Jr. et al., 2015), FCC risers (Rossbach et al., 2016), urea prilling towers (Ricardo et al., 2015), and many others.

One common benchmark case used to validate simulation codes is the horizontal pipe. A great number of data is provided in the literature for such case with various fluid inlet velocities, particles mass loadings, particles physical properties, and wall roughness (Tsuji et al., 1991; Huber and Sommerfeld, 1998). The experimental data of Huber and Sommerfeld (1998) is particularly interesting because many other works have used it for validation, e.g. Laín and Sommerfeld (2013) and Alletto and Breuer (2013).

Huber and Sommerfeld (1998) themselves and Alletto and Breuer (2013) presented simulation data for cases with different wall roughness and mass loading, with good agreement. Both studies used a direct contact handling of the collisions, which are very close to the physics but are computationally expensive. On the other hand Laín and Sommerfeld (2013) used a computationally cheap stochastic inter-particle collision model, which uses an analogy with the kinetic theory of gases to estimate the probability of collisions.

The objective of this work, is to perform a validation study of the in-house code UNSCYFL3D v2.3 with the aforementioned experimental data, using a distribution of diameters. This code uses a stochastic inter-particle collision model as well. The main goal is to check its performance in smooth and rough wall cases.

2. METHODOLOGY

In this section the mathematical and numerical methodology used by the in-house code UNSCYFL3D is described in a simplified manner. For more details about it, such as equations, models, correlations, algorithms and others, the reader is referred to journal publications using the software such as de Souza et al. (2014), for instance.

2.1 Gas phase model

An Unsteady-Reynolds-Averaged Navier-Stokes (URANS) approach is adopted, solving both mass and momentum equations for the gas phase. The turbulence closure is performed employing the *two-layer* k-ε model (Chen and Patel, 1988) and the Reynolds Stress Model (RSM). The grid has to be refined at the walls to ensure $y^+ = 1$.

The SIMPLE algorithm is used to couple the velocity and pressure fields. The collocated arrangement is used for all variables, with the conventional Rhie-Chow interpolation scheme for the computation of the mass flow rate through each element face. The discretization procedure described above generates a linear system of equations for each variable at each element center. The bi-conjugate gradient and the algebraic multigrid (AMG) methods are used to efficiently solve the linear system resulting from the discretization of the conserved and turbulence properties. The second-order upwind scheme was employed for the advective term, whereas the centered differencing scheme was used for the diffusive terms of the momentum equations and turbulence model equations.

2.2 Particle phase model

Three vector equations are solved to track the particles in a Lagrangian framework, the trajectory, linear momentum, and angular momentum equations. In the linear momentum equation the following forces are considered: drag force, with the CD coefficient calculated by Schiller and Naumann (1935) correlation; shear-induced lift force based on the analytical result of Saffman (1965) and extended for higher particle Reynolds numbers according to Mei (1992); the rotation-induced lift computed on the relation given by Rubinow and Keller (1961). The fluid velocity used in all correlations should be the instantaneous instead of the averaged, and so it is corrected using a Langevin dispersion model based on k and Îţ, locally. In the angular momentum equation the torque exerted from the fluid flow to the particle is given by Rubinow and Keller (1961) and extended by Dennis et al. (1980).

Inter-particle collisions are evaluated by a stochastic and hard-sphere model proposed by Oesterle and Petitjean (1993) and Sommerfeld (2001). For each computational particle, a fictitious collision partner is generated, and the probability of a collision is checked based on an analogy with the kinetic theory of gases. This requires that Gaussian distributions of velocity and diameter to be sampled and stored to generate the fictitious colliding partner. Nevertheless, whilst the original model suggests that one velocity distribution should be sampled for each diameter class, this model has been altered in the present work, sampling only one particle velocity distribution for all diameter classes in order to save computational memory. Some tests with the code proved that this simplification does not compromise the results for horizontal pipes.

Particle-wall collisions are handled according to the mechanistic equations of collision also, but a correction needs to be added to account for the wall surface roughness. The instantaneous impact angle is assumed to be composed by a particle trajectory angle plus a random component sampled from a Gaussian distribution function (Huber and Sommerfeld, 1998). This distribution has physical meaning and represents the standard deviation of the roughness angle distribution of the surface, which can be measured experimentally.

2.3 Numerical setup and procedure

Four cases were studied in this work, which are summarized in Tab. 1. For Case 1 (rough wall) the standard deviation of the roughness angle distribution of the surface was set to $10°$, as suggested by Laín and Sommerfeld (2013). For Case 2 the roughness parameter was tested with $0°$ and $1°$ to show the influence of this parameter. The remaining smooth wall cases are then simulated with a minor angle because of the results given in Case 2.

Table 1. Summary of simulations.

Case	Pipe diameter (mm)	Pipe length (m)	Conveying velocity (m/s)	Mass loading $(\mathrm{kg_{particle}}/\mathrm{kg_{air}})$	Mean particle diameter (µm)	Particle density $(\mathrm{kg/m^3})$	Wall surface
1 (1)	150	10.6	27	0.7	40	2500	Rough
2 (1)	80	5	24	0.3	40	2500	Smooth
3 (2)	30.5	3.56	15	0.4	210	1000	Smooth
4 (3)	63	6	20	1.0	130	2450	Smooth

(1) Huber and Sommerfeld (1998)
(2) Tsuji and Morikawa (1982)
(3) Laín and Sommerfeld (2012)

For all cases air phase physical properties were considered constant with density $\rho_f = 1.2\ \mathrm{kg/m^3}$ and viscosity $\mu_f = 1.8 \times 10^{-5}\ \mathrm{kg/(m\,s)}$. The particle size distribution was accounted for when available.

All numerical grid were generated in a similar manner, using only hexahedral cells (Fig. 1). Gradual refinement is employed near the walls, where great velocity gradients and boundary layer exist, also this is a requirement to get the most of the two-layer turbulence models. The grid resolution used in the simulations ranged from $400\,000$ to $600\,000$ depending on the pipe length, which were found to produce grid-independent results.

The UNSCYFL3D code is able to use different time-steps for the fluid and particle phase, and so the fluid equations are solved with 1×10^{-4} s and the particles with 1×10^{-5} s. Around five particle residence time were simulated to ensure a good sampling for mean values.

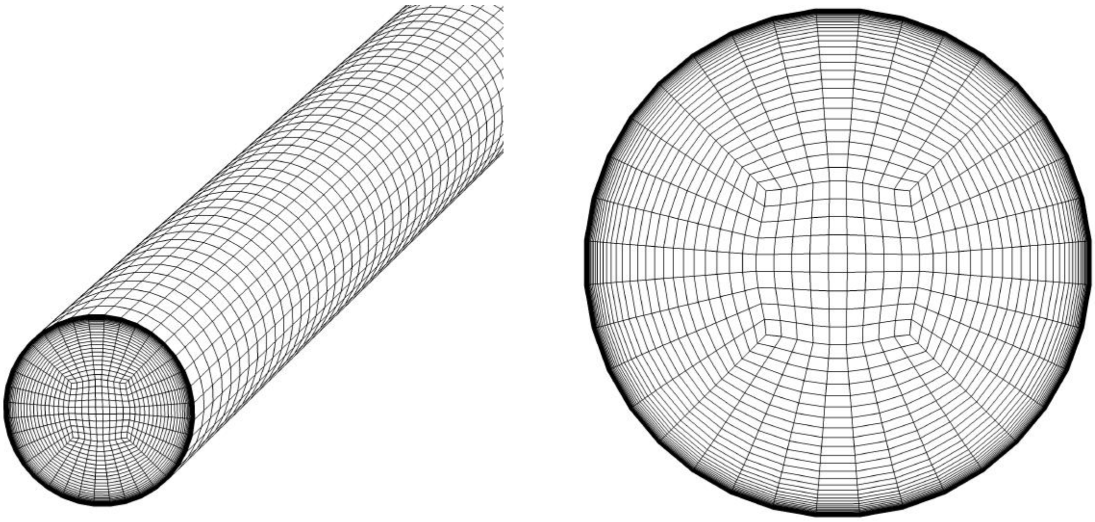

Figure 1. Numerical grid used in the pipe simulations: (left) isometric pipe view; (right) close view of the inlet.

3. RESULTS AND DISCUSSION

Particle velocity and diameter profiles for Case 1 (rough wall) are presented in Fig. 2. The results of two turbulence closure models are shown to compare with the experimental data from Huber and Sommerfeld (1998). Both models are able to provide good predictions for the mean velocity and mean diameter profiles. The RSM model has a slightly better agreement than the two-layer k-ε in the center region of the pipe for the velocity, but provides poorer agreement for the diameter in the central and upper region. For the rms velocity, both models display similar agreement. Some underprediction, mainly at the wall region, is expected and have been reported by others studies as well.

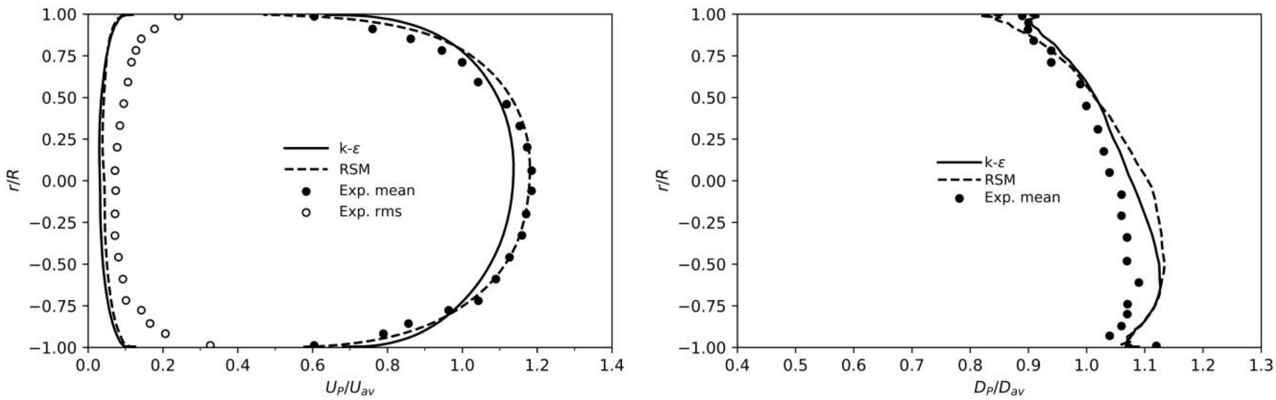

Figure 2. Particle velocity (left) and diameter (right) for simulation of Case 3 of Huber and Sommerfeld (1998), four-way coupling.

For Case 2, two values for wall roughness were use, the reasons why are clarified bellow. As the particle concentration maps in Fig. 3 show, when a 0° roughness is used, a annular region of high concentration is formed all around the pipe walls (Fig. 3-left), which is physically non-sound. A minor roughness needs to be used to correct for this behavior (Fig. 3-right), which is more coherent.

The phenomena attributed to the particles being stuck at the walls in cases with zero wall roughness, is the fact that the high fluid conveying velocity and low particle mass loading (leading to low collision probability), lead the particles to have a nearly parallel trajectory with very low transversal velocities after the flow is developed. As the particles approach the walls with very low angle of incidence, a very low angle of exit is generated, making them to not be able to get out of this low velocity region. They only can do so, when the incidence angle is corrected, even by a small value. Although this small angle correction may sound arbitrary, it is physically correct, because there is no wall truly smooth.

However the concentration maps are corrected using the small angle, the particle velocity profiles are not changed. Figure 4 show the velocity profiles for the two-layer k-ε model only, as it presented good accuracy in the last case. For the present case, however, a very poor agreement was obtained. The asymmetric profile with the great deficit in the bottom region is not predicted.

It is unclear why this specific case presents a bad agreement with experimental data, since the rough wall cases

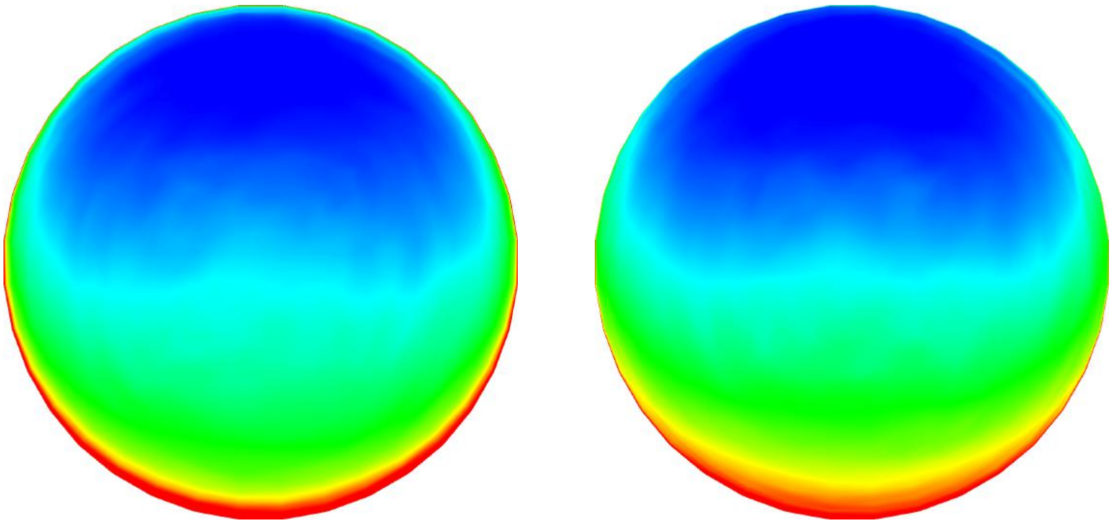

Figure 3. Particle concentration maps for a $0°$ (left) and $1°$ (right) wall roughness, simulation of Case 2 of Huber and Sommerfeld (1998), four-way coupling.

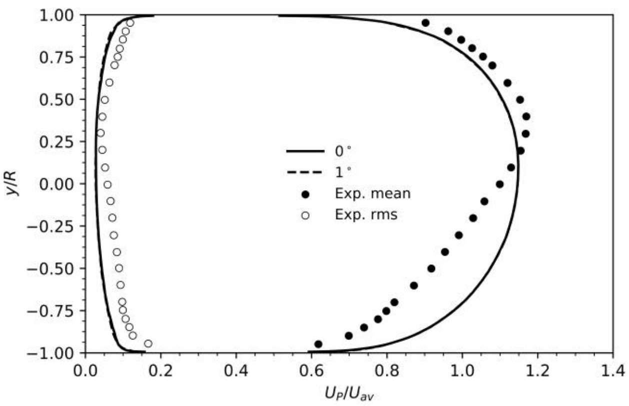

Figure 4. Particle average and rms velocity for a $0°$ and $1°$ wall roughness, simulation of Case 2 of Huber and Sommerfeld (1998), four-way coupling.

presented a very good one. To clarify whether this is a problem with the wall collision model treatment for smooth walls, another case with comparison of data from Tsuji and Morikawa (1982) is presented in Fig. 5. Comparison with fluid and particle velocity profiles are presented, and show a very good agreement as well. Note that they have similar mass loadings (0.3 and 0.4), but the latter case does not show the great deficit in the bottom region as in the former, and also almost no asymmetry.

A final simulation is presented in order to assess the matter of the particle velocity deficit in the bottom region of the pipe, namely Case 4. For this case, only the two-way coupling simulation is presented, which will give information about the influence of the particle phase on the velocity profiles. If a four-way coupling were to be used, a great redispersion of particles were to be seen (Laín and Sommerfeld, 2012), because of the not so low mass loading ($\eta = 1$), and symmetrical profiles similar to Case 1 would be achieved.

Fluid and particle velocity profiles are presented in Fig. 6 for the aforementioned case in comparison with simulation data from Laín and Sommerfeld (2012). A good agreement is obtained between the simulations, and both profiles show that the deficit of momentum in the bottom region is much less strong than in Case 2. Note that this case has a higher mass loading of particles with similar density, which should give rise to a higher, and not lower, deficit. In Case 4, the lowest particle velocity achieved in the bottom wall is around 80% of the average velocity, while in Case 2 is around 60%.

4. CONCLUSIONS

The results showed that the described methodology is very suitable for simulations of rough wall pipe flows, as have others confirmed (Huber and Sommerfeld, 1998; Sommerfeld, 2001). A poor agreement was achieved for a smooth wall case, with reasons unclear. However, other simulations of smooth wall cases confirmed that the same methodology can accurately predicts the fluid and particle velocity profiles for this flow as well.

Another conclusion is that even for smooth wall cases, a small angle has to be added to the model to account for the

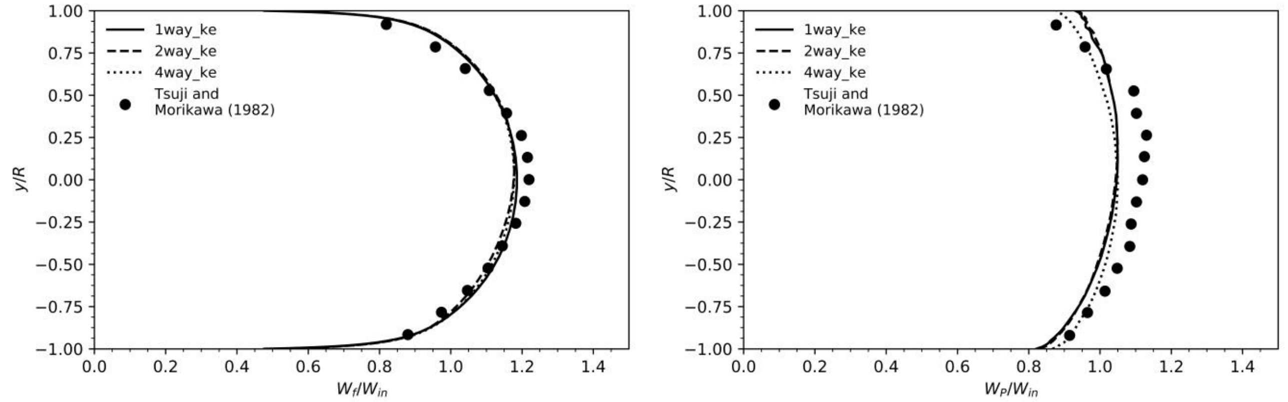

Figure 5. Fluid (left) and particle (right) velocity profiles in comparison with data from Tsuji and Morikawa (1982), four-way coupling.

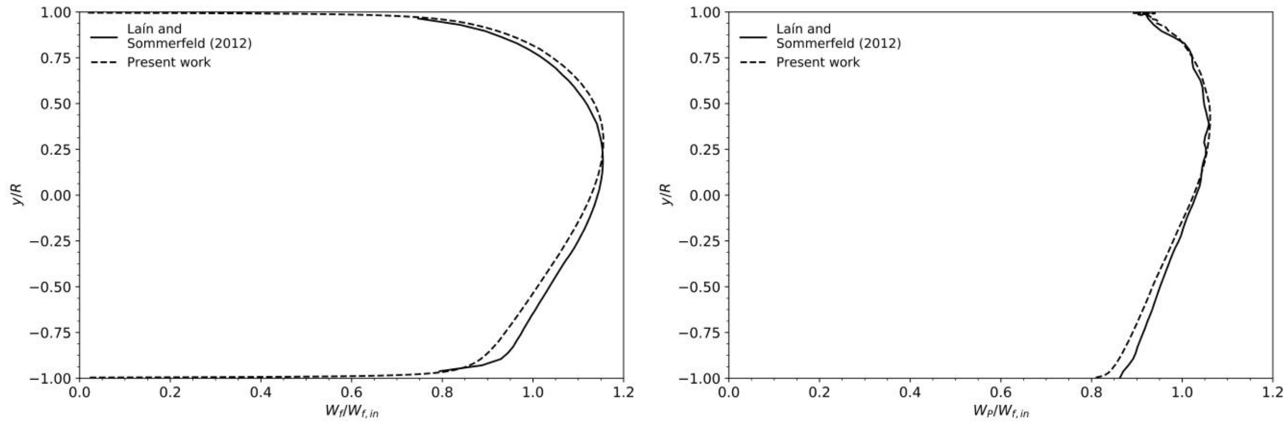

Figure 6. Fluid (left) and particle (right) velocity profiles in comparison with data from Laín and Sommerfeld (2012), two-way coupling.

fact that no surface is totally smooth. Using a value of 0° can make the particles get stuck in low velocity regions all around the wall, including in the upper region of the pipe.

5. ACKNOWLEDGEMENTS

The authors would like to thank the financial support of the Brazilian National Council of Technological and Scientific Development (CNPq) and the Foundation for Research Support of the State of Minas Gerais (FAPEMIG).

6. REFERENCES

Alletto, M. and Breuer, M. (2013). Prediction of turbulent particle-laden flow in horizontal smooth and rough pipes inducing secondary flow. *Int. J. Multiphas. Flow*, 55:80–98.

Chen, H. C. and Patel, V. C. (1988). Near-wall turbulence models for complex flows including separation. *AIAA J.*, 26(6):641–648.

de Souza, F. J., de Vasconcelos Salvo, R., and de Moro Martins, D. A. (2012). Large Eddy Simulation of the gas–particle flow in cyclone separators. *Sep. Purif. Technol.*, 94:61–70.

de Souza, F. J., Silva, A. L., and Utzig, J. (2014). Four-way coupled simulations of the gas–particle flow in a diffuser. *Powder Technol.*, 253:496–508.

Dennis, S. C. R., Singh, S. N., and Ingham, D. B. (1980). The steady flow due to a rotating sphere at low and moderate Reynolds numbers. *J. Fluid Mech.*, 101(02):257–279.

Duarte, C. A. R., de Souza, F. J., and dos Santos, V. F. (2016). Mitigating elbow erosion with a vortex chamber. *Powder Technol.*, 288:6–25.

Huber, N. and Sommerfeld, M. (1998). Modelling and numerical calculation of dilute-phase pneumatic conveying in pipe systems. *Powder Technol.*, 99(1):90–101.

Laín, S. and Sommerfeld, M. (2012). Numerical calculation of pneumatic conveying in horizontal channels and pipes: Detailed analysis of conveying behaviour. *Int. J. Multiphas. Flow*, 39:105–120.

Laín, S. and Sommerfeld, M. (2013). Characterisation of pneumatic conveying systems using the Euler/Lagrange approach. *Powder Technol.*, 235:764–782.

Mei, R. (1992). An approximate expression for the shear lift force on a spherical particle at finite Reynolds number. *Int. J. Multiphas. Flow*, 18(1):145–147.

Oesterle, B. and Petitjean, A. (1993). Simulation of particle-to-particle interactions in gas solid flows. *Int. J. Multiphas. Flow*, 19(1):199–211.

Ricardo, G. A. N., Noriler, D., Martignoni, W. P., and Meier, H. F. (2015). Application of Euler–Lagrange Approach to Predict the Droplet Solidification in a Prilling Tower. *Ind. Eng. Chem. Res.*, 54(39):9615–9626.

Rossbach, V., Utzig, J., Decker, R. K., Noriler, D., and Meier, H. F. (2016). Numerical gas-solid flow analysis of ring-baffled risers. *Powder Technol.*, 297:320–329.

Rubinow, S. I. and Keller, J. B. (1961). The transverse force on a spinning sphere moving in a viscous fluid. *J. Fluid Mech.*, 11(03):447–459.

Saffman, P. G. (1965). The lift on a small sphere in a slow shear flow. *J. Fluid Mech.*, 22(02):385–400.

Schiller, L. and Naumann, A. (1935). A drag coefficient correlation. *Z. Ver. Dtsch. Ing.*, 77:318–320.

Sedrez, T. A., Decker, R. K., da Silva, M. K., Noriler, D., and Meier, H. F. (2017). Experiments and CFD-based erosion modeling for gas-solids flow in cyclones. *Powder Technol.*, 311:120–131.

Sgrott Jr., O. L., Noriler, D., Wiggers, V. R., and Meier, H. F. (2015). Cyclone optimization by COMPLEX method and CFD simulation. *Powder Technol.*, 277:11–21.

Sommerfeld, M. (2001). Validation of a stochastic Lagrangian modelling approach for inter-particle collisions in homogeneous isotropic turbulence. *Int. J. Multiphas. Flow*, 27(10):1829–1858.

Tsuji, Y. and Morikawa, Y. (1982). LDV measurements of an air—solid two-phase flow in a horizontal pipe. *J. Fluid Mech.*, 120:385–409.

Tsuji, Y., Shen, N. Y., and Morikawa, Y. (1991). Lagrangian simulation of dilute gas-solid flows in a horizontal pipe. *Adv. Powder Technol.*, 2(1):63–81.

7. RESPONSIBILITY NOTICE

The authors are the only responsible for the printed material included in this paper.